

# A new supramolecular sulfonated polyimide for use in proton exchange membranes for fuel cells†

Yun-Sheng Ye, Yao-Jheng Huang, Chih-Chia Cheng and Feng-Chih Chang\*

Received 2nd July 2010, Accepted 24th August 2010

DOI: 10.1039/c0cc02325f

**Uracyl-terminated telechelic sulfonated polyimides (SPI-U) were transformed into noncovalent network membranes through biocomplementary hydrogen bonding recognition in the presence of an adenine-based crosslinking agent. SPI-U membrane exhibited dramatically improved methanol permeability, oxidative stability, proton conductivity, and selectivity relative to those of the standard SPI.**

Nonfluorinated polymeric materials are attracting increasing attention as alternatives to perfluorinated polymer membranes, such as Nafion or Aciplex, for use as proton exchange membranes (PEMs) in fuel cells, because of their advantages in terms of cost, monomer toxicity, ease of synthesis, and structural diversity.<sup>1</sup> Although nonfluorinated PEMs can achieve high proton conductivities when they feature a high content of sulfonic acid groups, such systems tend to exhibit poor mechanical strength and low permeability. The development of more efficient membranes exhibiting improved proton conductivity and reduced methanol crossover, without detrimentally affecting the mechanical and chemical stabilities, remains a challenge.<sup>2</sup> One effective way to enhance PEM performance is to distinctly separate the hydrophilic sulfonic acid group regions from the hydrophobic polymer main chains by locating the sulfonic acid groups on side chains through grafting onto the polymer main chains.<sup>3</sup> In addition, tethering of N-heterocycles to a polymer backbone, followed by blending with a sulfonic acid polymer, is an attractive strategy to achieve high PEM performance through acid–base interactions between the sulfonic acid groups in one (acidic) polymer and the N-atom-containing groups in the other (basic) polymer.<sup>4</sup> Another strategy for improving the PEM performance is to generate uniformly distributed hydrophilic conductive sites and then control the hydrophobic nature by minimized crosslinking over the sulfonated polymer structure.<sup>5</sup>

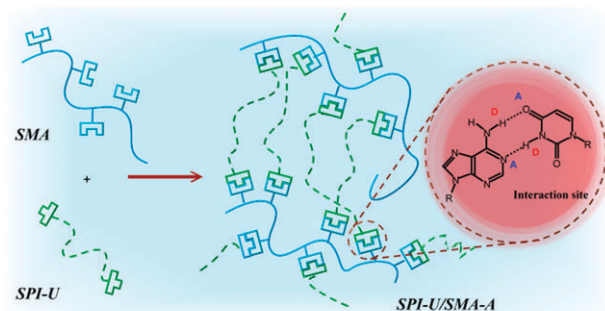
Noncovalent crosslinking offers several novel strategies for materials design, because noncovalent crosslinking is inherently reversible, highly tunable, avoids potential side reactions (*e.g.*, chain degradation), and provides unlimited processability.<sup>6</sup> Hydrogen bonding is the most common noncovalent interaction used to produce reversible crosslinked polymeric networks.<sup>7–9</sup> Generally, polymeric networks based on hydrogen bonding can be classified into two broad classes: those formed through self-association<sup>8</sup> and those formed through the addition of an

external crosslinking agent.<sup>9</sup> In self-associative systems, inter-chain crosslinking (*e.g.*, dimerization) provides great control over the network structure, but the degree and strength of the crosslinks are difficult to control. In the second category, the degree and strength of the crosslinks can be tuned by varying the amount or type of crosslinking agent. Recently, we demonstrated that it is possible to form DNA-like side-chain polymers by choosing biocomplementary hydrogen bonding recognition units (thymine–adenine; T·A),<sup>10</sup> thereby providing a potential route to the design of new molecular architectures in supramolecular polymers.

In this study, we prepared a uracyl-terminated telechelic sulfonated polyimide (SPI-U) and transformed it into noncovalent network membranes through biocomplementary hydrogen bonding recognition in the presence of an adenine-based crosslinking agent (SMA-A; Scheme 1).

We synthesized the SMA-A crosslinking agent (polymer 7) from monomer 1 in four steps (Scheme S1, ESI†). The synthesis of the SPI-U (polymer 8) involved three steps (Scheme S2, ESI†): an anhydride-terminated sulfonated polyamic acid (PAA) was synthesized using a slight excess of NTDA in the copolymerization reaction, the terminal anhydride groups were end-capped with uracyl (monomer 4) to produce a uracyl-terminated PAA, and then the SPI-U was obtained after thermal imidization. The theoretical molecular weight of the SPI-U was calculated by comparing the integrals of the signals of the uracyl and naphthene groups in its <sup>1</sup>H NMR spectrum (25 °C, DMSO-*d*<sub>6</sub>). The copolymer composition (*n* : *m*) was confirmed by the relative <sup>1</sup>H NMR spectroscopic absorption peak areas of signals *j* and *i* in Fig. S7 (ESI†). The properties of the SPI-U and the standard SPI containing 80% hydrophilic units (*n* : *m* = 8 : 2) is the focus of this Communication.

Before conducting crosslinking studies, we first investigated (Fig. 1) the biocomplementary (U·A) hydrogen bonding recognition between the SPI-U and the adenine compound



**Scheme 1** Graphical representation of a crosslinked SPI-U/SMA-A complex.

Institute of Applied Chemistry, National Chiao-Tung University, Hsin-Chu, Taiwan. E-mail: changfc@mail.nctu.edu.tw; Tel: +886 03 57131512

† Electronic supplementary information (ESI) available: Details of experiment, NMR spectra and membrane properties. See DOI: 10.1039/c0cc02325f

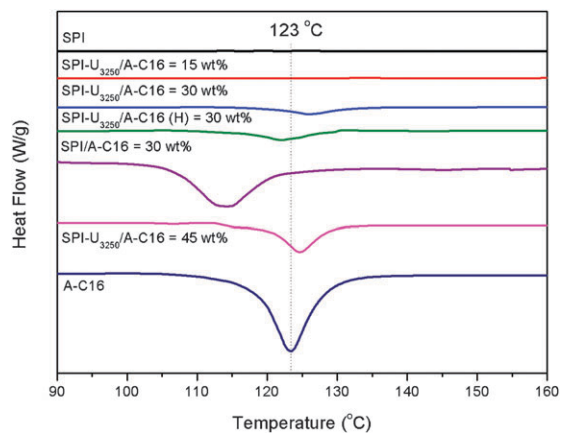


**Fig. 1** DSC curves of SPI and SPI-U<sub>3250</sub> samples containing various amounts of A-C16.

A-C16 using differential scanning calorimetry (DSC). To monitor the thermal transitions more clearly, we used an SPI-U of lower theoretical molecular weight [SPI-U<sub>3250</sub>; Fig. S7 (a), ESI†] in these studies. The value of  $T_m$  of the pure A-C16 was 123 °C; neither SPI nor SPI-U<sub>3250</sub> exhibited a value of  $T_m$ . For the complex formed from SPI-U<sub>3250</sub> and 15 wt% A-C16, we did not observe a value of  $T_m$  for A-C16, indicating that the uracil groups of SPI-U<sub>3250</sub> were highly complementary to the adenine groups of A-C16. The use of 30 wt% A-C16 resulted in a slightly visible peak at 128.6 °C, suggesting the presence of a slight excess of A-C16 in the SPI-U<sub>3250</sub>/A-C16 complex. We obtained similar results after converting the SPI-U<sub>3250</sub>/A-C16 complex into its highly dissociable sulfonic acid form, indicating that SPI-U<sub>3250</sub> and A-C16 formed highly stable hydrogen-bonded complexes in the bulk state. In contrast, when the SPI was blended with 30 wt% A-C16, we obtained an obviously lower value of  $T_m$ . Wide-angle X-ray diffraction (WAXD) patterns of pure SPI and pure SPI-U display (Fig. S8, ESI†) several amorphous halos (26.0° for SPI; 26.0, 15.5, 8.3, and 6.6° for SPI-U). When U···A interactions were present, the characteristic peak of A-C16 disappeared and the amorphous halo of SPI-U<sub>3250</sub> ( $2\theta = 26.0^\circ$ ) shifted to a lower value; in contrast, the characteristic peaks of A-C16 ( $2\theta = 3.2$  and  $3.5^\circ$ ) remained in the case of the SPI/A-C16 complex.

After conducting these preliminary biocomplementary hydrogen bonding recognition studies, we tested the crosslinking of SPI-U with the adenine-based crosslinking agent SMA-A. The solution of SPI-U (at 30 wt% solid content) was a low-viscosity fluid that readily flowed when we inverted the vial; in contrast, the SPI-U crosslinked with 20 wt% SMA-A was an elastic solid. The left-hand image in Fig. S9 (ESI†) presents the vial-inversion experiment performed using 10 wt% SMA-A; the gel did not flow after several minutes at room temperature, but it did flow gradually after several hours. The right-hand image in Fig. S9 (ESI†) presents the crosslinked SPI-U/SMA-A fluid after heating at 80 °C, a temperature at which the gel fluid was transformed into a low-viscosity fluid. The variation in flow behavior indicates that the degree of crosslinking can be tuned by varying the amount of the crosslinking agent. Similar results were verified in viscosity measurements of the SPI/SMA-A and the SPI-U/SMA-A

blends (Fig. S10, ESI†). These two sets of blends exhibited opposite trends, confirming that hydrogen bonding was indeed occurring in this biocomplementary system.

Thermogravimetric analysis (TGA) revealed two-step weight losses for sulfonated polymer membranes (Fig. S11, ESI†). We observed slight increases of the first decomposition temperatures for the SPI/SMA-A and SPI-U/SMA-A membranes relative to pure SPI, implying that the sulfonic acid groups were more tightly held by the SPI/SMA-A and SPI-U/SMA-A membranes. We tested the oxidative stability of the prepared membranes using Fenton's reagent (30 wt% H<sub>2</sub>O<sub>2</sub> and 30 ppm FeSO<sub>4</sub>) at 30 °C (Table S1, ESI†). The oxidative stability of the blended membranes improved upon adding the adenine-based polymer because the acid–base interaction between the sulfonated polymer and SMA-A<sup>3,10</sup> retarded the permeation of H<sub>2</sub>O<sub>2</sub> through the membrane and decreased the rate of decomposition of the backbone aromatic units. Therefore, the formation of the supramolecular cross-linked structure resulted in improved oxidative stability relative to that of the unmodified SPI.

The type of crosslinking agent, the crosslinking density, and the microstructural change that occurs after crosslinking all have dramatic effects on the water uptake, the state of water, and the proton conductivity of crosslinked membranes. Although the addition of SMA-A to SPI-U resulted in reduced ion exchange capacity (IEC), water uptake (WU), and proton conductivity at 30 °C and 90% RH (Table S2, ESI†), the SPI-U/SMA-A exhibited higher proton conductivity (0.15 S cm<sup>-1</sup>) at 80 °C and 90% RH relative to those of the SPI (0.14 S cm<sup>-1</sup>) and the SPI/SMA-A (0.12 S cm<sup>-1</sup>) under the same conditions. According to the Arrhenius law, the temperature dependence of conductivity is associated with the activation process of proton conduction. The activation energies ( $E_a$ ) for the SPI, SPI/SMA-A, and SPI-U/SMA-A membranes at 90% RH were 10.8, 16.8, and 14.8 kJ mol<sup>-1</sup>, respectively; when the RH decreased from 90 to 50%, the values of  $E_a$  of both blended membranes (SPI/SMA-A and SPI-U/SMA-A) for unblended native SPI nearly doubled. These results indicate that a Grotthuss-type mechanism is predominant in both of the blended membranes under 50% RH conditions. Moreover, at 50% RH, both blended membranes displayed proton conductivities higher than those of SPI at temperatures between 30 and 80 °C (Fig. 2), implying that the incorporation of the adenine-based SMA-A into the membranes improved proton conduction at low RH, due to the hopping of protons between the sulfonic acid groups of the sulfonated polymer and the nitrogen atoms of SMA-A.<sup>4,10,11</sup> We obtained similar results from proton conductivity measurements performed under anhydrous conditions (Fig. S12, ESI†). Notably, the SPI-U/SMA-A membrane exhibited a more significant increase in proton conductivity upon increasing temperature at the various RH levels relative to those of the SPI and SPI/SMA-A membranes. This behavior arose presumably because the minimized network structure suppressed ionic cluster formation and resulted in a homogeneous distribution of the conductive sites over the polymer backbone.<sup>5</sup> TEM micrographs of the SPI and SPI-U/SMA-A membranes (Fig. 3) verified that the addition of SMA-A resulted in a better distribution of ionic clusters.

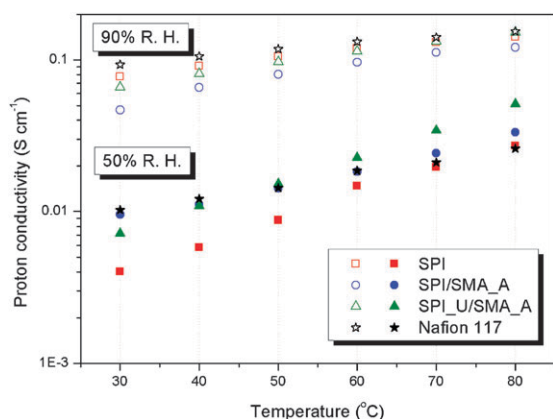


**Fig. 2** Temperature dependence of the proton conductivities for the SPI, SPI/SMA-A, and crosslinked SPI-U/SMA-A membranes at 50 and 90% RH.

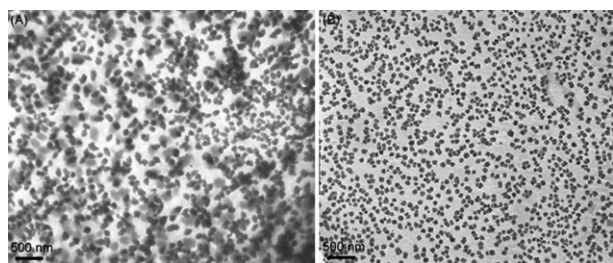


**Fig. 3** TEM micrographs of the (A) SPI and (B) SPI-U/SMA-A membranes.

Table S1 (ESI<sup>†</sup>) reveals that both blended membranes had lower methanol diffusion coefficients relative to that of the SPI membrane, with an especially significantly lower value for the crosslinked SPI-U/SMA-A membrane. The incorporation of the adenine-based SMA-A into the SPI or SPI-U caused the pendent adenine groups to insert into the sulfonic acid domains of the SPI or SPI-U, thereby retarding methanol crossover. Moreover, the presence of the crosslinking agent between the polymer chains prevented excessive water swelling while simultaneously retarding the degree of methanol crossover.<sup>4</sup> The methanol permeability of the SPI-U/SMA-A membrane was only 11% and 7% of that of the SPI membrane and Nafion 117 under the same conditions, respectively ( $0.94 \times 10^{-7} \text{ cm}^2 \text{ s}^{-1}$  for SPI-U/SMA-A,  $8.52 \times 10^{-7} \text{ cm}^2 \text{ s}^{-1}$  for SPI,  $13.1 \times 10^{-7} \text{ cm}^2 \text{ s}^{-1}$  for Nafion 117). The ratio of the proton conductivity to the methanol permeability—i.e., the selectivity ( $\Phi$ )—is an effective parameter for evaluating membrane performance in DMFCs. Table S1 (ESI<sup>†</sup>) indicates that the selectivity of the crosslinked supramolecular SPI-U/SMA-A membrane was approximately five and seven

times higher than that of the standard SPI and Nafion 117, respectively.

In summary, we have synthesized a new type of PEM comprising an SPI hydrogen-bonded with an adenine-based crosslinking agent. Compared with the pure SPI, both the SPI/SMA-A and SPI-U/SMA-A membranes exhibited improved properties: higher proton conductivities at high temperature and low RH, lower methanol permeabilities, and higher oxidative stabilities; the latter blend (SPI-U/SMA-A) is more favorable for membrane performance in DMFCs. We believe that this technique based on noncovalent interactions should be applicable to other hydrocarbon-based polymer membranes, thereby providing a useful method for improving the properties of PEMs.

## Notes and references

- (a) M. A. Hickner, H. Ghassemi, Y. S. Kim, B. R. Einsla and J. E. McGrath, *Chem. Rev.*, 2004, **104**, 4587; (b) B. C. H. Steele and A. Heinzl, *Nature*, 2001, **414**, 345; (c) C. Y. Wang, *Chem. Rev.*, 2004, **104**, 4727.
- (a) Y. Woo, S. Y. Oh, Y. S. Kang and B. Jung, *J. Membr. Sci.*, 2003, **220**, 31; (b) Y. S. Ye, W. Y. Chen, Y. J. Huang, M. Y. Cheng, Y. C. Yen, C. C. Cheng and F. C. Chang, *J. Membr. Sci.*, 2010, **362**, 29; (c) H. Tang, M. Pan, S. Lu, J. Lu and S. P. Jiang, *Chem. Commun.*, 2010, **46**, 4351.
- (a) B. R. Einsla and J. E. McGrath, *Am. Chem. Soc. Div. Fuel Chem.*, 2004, **49**, 616; (b) K. Miyatake, Y. Chikashige, E. Higuchi and M. Watanabe, *J. Am. Chem. Soc.*, 2007, **129**, 3879; (c) D. S. Kim, G. P. Robertson and M. D. Guiver, *Macromolecules*, 2008, **41**, 2126.
- (a) Y. Fu, A. Manthiram and M. D. Guiver, *J. Electrochem. Soc.*, 2007, **9**, 905; (b) Y. Fu, W. Li and A. Manthiram, *J. Membr. Sci.*, 2008, **310**, 262; (c) W. Li, A. Bellay, Y. Z. Fu and A. Manthiram, *J. Power Sources*, 2008, **180**, 719.
- (a) Y. Yin, S. Hayashi, O. Yamada, H. Kita and K. I. Okamoto, *Macromol. Rapid Commun.*, 2005, **26**, 696; (b) Y. S. Oh, H. J. Lee, M. Yoo, H. J. Kim, J. Han, K. Kim, J. D. Hong and T. H. Kim, *Chem. Commun.*, 2008, 2028.
- D. Bogdal, P. Perez, J. Pielichowski and A. Prociak, *Adv. Polym. Sci.*, 2003, **163**, 193.
- (a) T. Park and S. S. Zimmerman, *J. Am. Chem. Soc.*, 2006, **128**, 11582; (b) G. Cooke and V. M. Rotello, *Chem. Soc. Rev.*, 2002, **31**, 275.
- (a) L. L. De Lucca Freitas and R. Stadler, *Macromolecules*, 1987, **20**, 2478; (b) C. Hilger, M. Draeger and R. Stadler, *Macromolecules*, 1992, **25**, 2498; (c) L. R. Rieth, R. F. Eaton and G. W. Coates, *Angew. Chem., Int. Ed.*, 2001, **40**, 2153.
- (a) R. J. Thibault, P. J. Hotchkiss, M. Gray and V. M. Rotello, *J. Am. Chem. Soc.*, 2003, **125**, 11249; (b) T. Kawakami and T. Kato, *Macromolecules*, 1998, **31**, 4475; (c) K. P. Nair, V. Breedveld and M. Weck, *Macromolecules*, 2008, **41**, 3429.
- C. C. Cheng, Y. C. Yen, Y. S. Ye and F. C. Chang, *J. Polym. Sci., Part A: Polym. Chem.*, 2009, **47**, 6388.
- (a) J. Saito, K. Miyatake and M. Watanabe, *Macromolecules*, 2008, **41**, 2415; (b) J. Wang, Y. Song, C. Zhang, Z. Ye, H. Liu, M. H. Lee, D. Wang and J. Ji, *Macromol. Chem. Phys.*, 2008, **209**, 1495; (c) E. K. Pefkianakis, V. Deimede, M. K. Daletou, N. Gourdoupi and J. K. Kallitsis, *Macromol. Rapid Commun.*, 2005, **26**, 1724.